1995-05-15

The effect of salinity on density in the California Current system

Batteen, Mary L.

Journal of Geophysical Research, Vol. 100, No. C5, pp. 8733-8749, May 15, 1995
http://hdl.handle.net/10945/47163

JOURNAL OF GEOPHYSICAL RESEARCH, VOL. 100, NO. C5, PAGES 8733–8749, MAY 15, 1995

The effect of salinity on density in the California Current system

Mary L. Batteen, Curtis A. Collins, Christopher R. Gunderson,[1]
and Craig S. Nelson

Department of Oceanography, Naval Postgraduate School, Monterey, California

Abstract. There are some indications that in large measure the density anomaly field of the California Current system (CCS) follows temperature, salinity playing a significantly lesser role. These indications have been used as justification for not taking as extensive salinity as temperature observations in the CCS, as well as for using fixed or prescribed salinity fields in density calculations in dynamic models of the CCS. An extensive data base of temperature-salinity observations from the CCS is used to show that there are noticeable differences between the dynamic height field calculated with and without the inclusion of salinity variations. Hence the distribution of salinity is important in defining the large-scale circulation of the CCS. In particular, owing to the combined effect of temperature and salinity on density, the dynamic height fields show a significant equatorward component along the coast of California and a strong offshore component adjacent to Baja California. Based on these observations, it is concluded that descriptively and dynamically, both temperature and salinity are essential to accurately characterize the large-scale structure of the CCS.

1. Introduction

At a given pressure, the density of seawater depends on temperature and salinity. Except for high-latitude regions and near sources and sinks of salt, temperature is usually considered to vary more than salinity in the upper ocean and is generally considered to be the major source of density variations [*Pickard and Emery*, 1990]. Recently, *Cooper* [1988] demonstrated the importance of salinity to density variations in modeling motions in the tropics. Is it possible that salinity variability in the California Current system (CCS), which geographically lies between the polar regions and the tropics, is also an important consideration to density variations? A close examination of the southern CCS area in Figure 1 of *Cooper* [1988] suggests that salinity variations could have as important an effect in the CCS as in the tropics.

In the CCS, unlike all other eastern boundary currents, salinity increases rather than decreases with depth [*Wooster and Reid*, 1963]. This anomalous feature can result in significantly denser water upwelled to the surface. For example, examination of Figures 18–20 of *Huyer and Kosro* [1987], which depict the coastal area of the CCS just north of Point Arena (at ~39°N), shows that at a depth of 100 m about a third of the cross-shore density gradient over a degree of longitude is due to salinity change. Near the coast, cold, salty 100-m water is upwelled to the surface, resulting in horizontal density gradients that are at least one third greater than if the salinity profile did not change with longitude.

An approximate equation of state for seawater is

$$\rho = \rho_0[1 - \alpha(T - T_0) + \beta(S - S_0)], \quad (1)$$

which can be rewritten as

$$\Delta\rho = -\alpha\rho_0\Delta T + \beta\rho_0\Delta S, \quad (2)$$

where α and β are the expansion and contraction coefficients for temperature T and salinity S, respectively, ρ is density, S_0 is the reference salinity (35 psu (practical salinity units)), and T_0 is the reference temperature (0°C). This equation can estimate the effect of salinity for the entire region if typical CCS values for T and S are used. From the International Oceanographic Tables [*UNESCO*, 1987] for α and β with 15°C and 33 psu, and considering typical surface temperature and salinity ranges of 10°C and 2 psu for the CCS, computations of the contributions of temperature and salinity to the density anomaly are 10.5 and 7.5 kg m^{-3}, respectively. For a smaller area, a mean temperature of 13°C ± 2°C variation, associated with a mean salinity of 33.3 with a standard deviation of 0.3 psu, is roughly characteristic of the central region of the CCS [*Lynn et al.*, 1982]. Use of the 1987 tables here shows a contribution of 2.7 and 1.7 kg m^{-3} to the annual density anomaly change for temperature and salinity, respectively, over the course of a year. Vertically a mean temperature at 500 m of about 5°C ± 5°C surface to 1000 m, in conjunction with an approximate mean salinity of 34 ± 0.5 psu, yields density anomaly changes of 7.2 kg m^{-3} from temperature and 3.8 kg m^{-3} from salinity.

These estimates indicate that the importance of salinity variation should not be summarily dismissed when considering CCS density gradients in any dimension. Yet often dynamic models of the CCS use a fixed salinity field (e.g., *Batteen et al.* [1989] in a model of the central CCS) and thus do not allow salinity contributions to density gradients. Furthermore, the salinity field has often been inferred (e.g., from expendable bathythermograph (XBT) observations [e.g., *Rienecker et al.*, 1985]) rather than directly measured.

Since the effect of salinity gradients on the large-scale ocean circulation of the CCS has not been previously evaluated, the objective of this study is to assess this effect by comparing dynamic height fields calculated with and without

[1]Now at Oceanography Department, U.S. Naval Academy, Annapolis, Maryland.

Paper number 95JC00424.

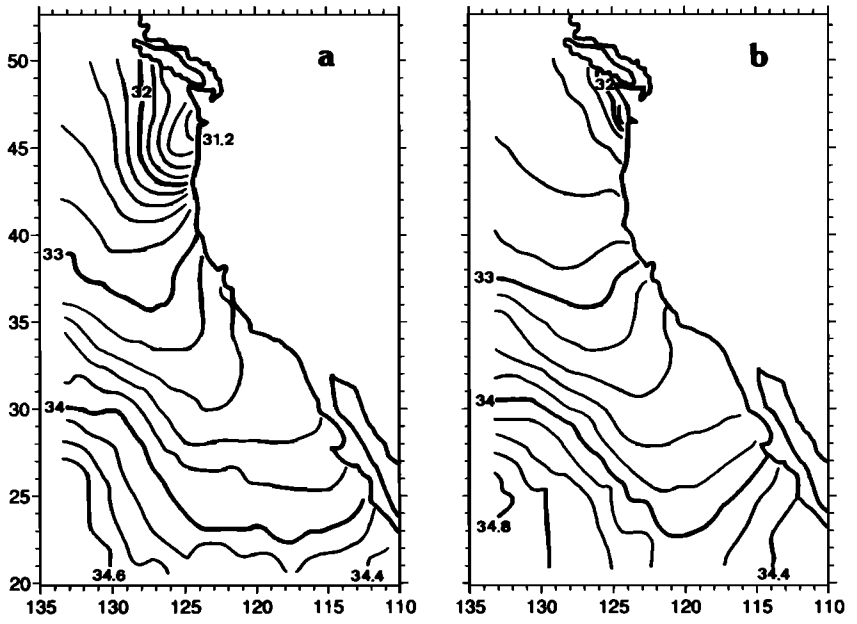

Figure 1. Surface salinity of the California Current system in (a) summer and (b) winter (adapted from *Blumberg et al.*, [1984]). The contour interval is 0.2 psu (practical salinity units).

the inclusion of salinity variations. The data set used is described in section 2. Using this data set, a brief presentation of the characteristic salinity fields of the CCS is provided in section 3. In section 4, mean dynamic heights are computed from salinity and temperature observations and are compared with dynamic heights computed from temperature and constant salinity values. To show the effect of salinity gradients, the difference between the two dynamic height fields is also calculated. A summary of the results and a discussion of modeling implications are presented in section 5.

2. Data Description

The data base used for all calculations was compiled by Dynalysis of Princeton and is described in detail by *Blumberg et al.* [1984]. Coverage extends along the west coast of North America to 133°W and from 20° to 50°N. Sources include the National Oceanographic Data Center (NODC) data archives, the Fleet Numerical Oceanography Center (FNOC) data files, California Cooperative Oceanic Fisheries Investigation (CalCOFI) surveys made systematically since 1949, and the Coastal Ocean Dynamics Experiment (CODE) data. The combined data set consists of over 300,000 data points with observations at up to 33 standard levels to 4000 m. The more than 40,000 of these points which included any simultaneous temperature and salinity observations at 500 m or above were considered here, while those including only temperature were not used. The CalCOFI collection defines for the most part the maximum resolution possible from the data set, exceptions being along the Oregon coast and near Point Arena, where finer resolution may be possible. Generally, the number of observations increases toward the coast, with greatest concentration along the coasts of California and Oregon. There are very few data more than 500 km off the coast or between 38° and 42°N. Discussion here is limited to the area bounded by the extent of these data.

For this study, data were placed in bins identified by 1° squares centered at half degree latitude-longitude intersections, by month, and by depth level. The numbers of observations associated with each data block are plotted by *Gunderson et al.* [1989]. The choice of 500 m as the maximum depth level was due to data availability and because the phenomenon of interest, the CCS, has been classically considered shallower than that depth, at least within 300 km of shore [*Hickey*, 1979]. The choice of 1° squares was again due to data availability; the CalCOFI sampling grid does not support finer resolution. For the dynamic height calculations, only casts that include temperature and salinity data at all standard depths from the surface to 500 m were used.

3. Characteristic Salinity of the CCS

Maps of the sea surface salinity, obtained from the data set for summer (Figure 1a) and for winter (Figure 1b), show that the sea surface salinity generally increases from about 32 psu near the Washington-Canada border to about 34 psu near Baja California. At a given latitude, salinity tends to be maximum at the coast, decreases offshore, then increases again at the western limits of the CCS. That is, the isohalines describe a trough, the axis of which extends from the coast near the mouth of the Columbia River near 46°15'N to a point about 500 km off the coast at Baja California. In the southwest corner of the CCS, approximately 700 km off the coast, the isohalines are oriented northwest-southeast with a relatively tight gradient, of the order of 0.1 psu in 40 km.

The most dramatic seasonal change to the surface salinity in the CCS results from river discharge. During the summer (Figure 1a), important sources of fresh water runoff along the West Coast are the Fraser River, which discharges through the Straits of Georgia and Juan de Fuca at 48°30'N, and the Columbia River at 46°15'N. The Fraser's fresh water is mixed deep, and its signature is lost, but as *Huyer* [1983] first noted, the direct effect of the Columbia is visible as far south

as San Francisco. During spring (not shown) an area of tight isohaline spacing, roughly 0.1 psu in 30 km, exists within a radius of ~500 km of the Columbia's mouth. Through the course of a year the area of tight gradient gradually decreases until by winter (Figure 1b) the strong gradient exists only in the immediate vicinity of the mouth of the river and northward along the coast of Washington.

Consistent with *Huyer* [1983] and *Emery and Dewar* [1982], typical profiles are marked by permanent haloclines: sharp and shallow (150 m) in the north, and less distinct and deeper (200 m) to the south. At 500-m depth the mean salinity increases from 34.1 psu near 50°N to 34.5 psu near 20°N.

4. Analysis of Dynamic Height Patterns

Dynamic height anomaly $\Delta\Phi$ was calculated by integrating the specific volume anomaly δ over depth and comparing it with $\Delta\Phi_{35TP}$ (where the subscripts 35, T, and P stand for salinity 35 psu, temperature, and pressure, respectively), calculated by integrating δ_T. To show the effect of salinity gradients, dynamic difference fields $\Delta\Phi'$ (where $\Delta\Phi' = \Delta\Phi - \Delta\Phi_{35TP}$) were also calculated. Comparisons between horizontal gradients of $\Delta\Phi$ and $\Delta\Phi_{35TP}$ are used to provide insight concerning the importance of salinity variations to the flow field, while the $\Delta\Phi'$ patterns define mean geostrophic flow that will not be accounted for if δ_T alone is used as an indicator of δ. Note that the magnitude of $\Delta\Phi_{35TP}$ (and hence $\Delta\Phi'$) is associated with the choice of a reference salinity but gradients are not. The choice of 35 psu was used so that our results could be compared with those of similar investigations, such as that of *Cooper* [1988].

Monthly mean values of $\Delta\Phi$, $\Delta\Phi_{35TP}$, and $\Delta\Phi'$, obtained by integrating from an assumed layer of no motion at 500 m to 200 m (200/500) and the surface (0/500) are shown in Figures 2–7. Note that the 0/500 plots for $\Delta\Phi$, $\Delta\Phi_{35TP}$, and $\Delta\Phi'$ (Figures 2–4) show gaps in the data off northern California, while the 200/500 plots for $\Delta\Phi$, $\Delta\Phi_{35TP}$, and $\Delta\Phi'$ (Figures 5–7) show gaps off southern Oregon and northern California.

4.1. Dynamic Height Patterns at 0/500

Examination of the 0/500 dynamic height fields of the CCS (Figure 2) shows that the total range of dynamic height varies from about 70 to 100 dyn. cm. Typically, the minimum dynamic height, less than 82 dyn. cm, is found at the coast off central California as well as at the northern extreme of our charts off Vancouver Island and the Strait of Juan de Fuca. In the north, this disappears in July–September. Off central California, the area encompassed by the 82 dyn. cm isostere is greatest from May through July, extending from Cape Blanco to the Southern California Bight area. The area shrinks to a minimum in November which is centered at Point Reyes, moves somewhat to the south and offshore in January and February, and returns to the coast south of Monterey in March. Relative minima are also found at Punta Eugenia (28°N) in June, July, September, and February.

The pattern of isosteres shown in Figure 2 is strongly parallel to the coast, associated with the southward flow of the California Current. The tendency for northward flow at the coast appears most frequently in the region of the Southern California Bight, associated with the circulation pattern of the southern California eddy. Off central California, evidence for poleward flow at the coast is confined to January and February when the minimum in dynamic height is offshore, as noted above.

Analysis of the $\Delta\Phi_{35TP}$ fields at 0/500 (Figure 3) shows that the isosteres associated with temperature change increase equatorward from about 30 to 70 dyn. cm. In fall and winter they have a zonal orientation, implying a geostrophic flow toward the coast. In spring and summer these isosteres acquire a more southeasterly tilt, especially in the region to the south of central California. The 42–50 dyn. cm isosteres, which occur in the region of central California, usually indicate a poleward bend at the coast which is associated with an offshore minimum in dynamic height.

Examination of the $\Delta\Phi'$ fields at 0/500 (Figure 4) shows that the isosteres associated with both temperature and salinity change increase poleward from about 24 to 50 dyn. cm and appear to be oriented perpendicular to shore, although the 36–44 dyn. cm isosteres usually bend poleward as they approach the coast, associated with a maximum or ridge in dynamic height offshore. During the period from September through January, a minimum in dynamic height, less than 36 dyn. cm, occurs between San Francisco and Point Conception. Although the overall pattern has only about 60% of the range in the change of dynamic height associated with temperature, it is important to note that the change of dynamic height associated with both temperature and salinity is opposite to that determined from the temperature field alone, i.e., equatorward flow at the coast with offshore flow implied over the entire domain.

4.2. Dynamic Height Patterns at 200/500

This is the level at which the undercurrent appears clearly. Analysis of the $\Delta\Phi$ fields at 200/500 (Figure 5) shows that the poleward flow is associated with the development of a dynamic trough off the California coast. Offshore, the isosteres are oriented parallel to the coast, consistent with equatorward flow of the California Current, with dynamic height increasing equatorward. In these charts, the 40 dyn. cm contour is found next to the coast in the region off central and southern California. Inshore, a well-developed poleward flow is indicated in January, February, July, August, and October by a retroflection of this isostere, corresponding to development of the dynamic trough. Except in April, May, and June, the dynamic height at the coast exceeds 40 dyn. cm in the region of the Southern California Bight, indicating poleward flow there, also associated with the undercurrent. In March, August, and September the dynamic trough is not continuous in the region off California, indicating the development of eddylike features. This may be due to seasonal heating and cooling.

The region between northern California and British Columbia is associated with the divergence of the North Pacific Current. The 38 dyn. cm isostere is indicative of this, indicating flow into the coast of Washington. In August, October, and November a cyclonic eddy (one data point) is found to the west of Punta Eugenia.

Examination of the Φ_{35TP} fields at 200/500 (Figure 6) shows that the isosteres associated with temperature variability alone also increase equatorward, from about 16 to 32 dyn. cm. The pattern of these isosteres differs dramatically from the previous picture in the region off Baja California, where the isosteres are oriented perpendicular to the coast and have a pronounced alongshore gradient, i.e., increasing

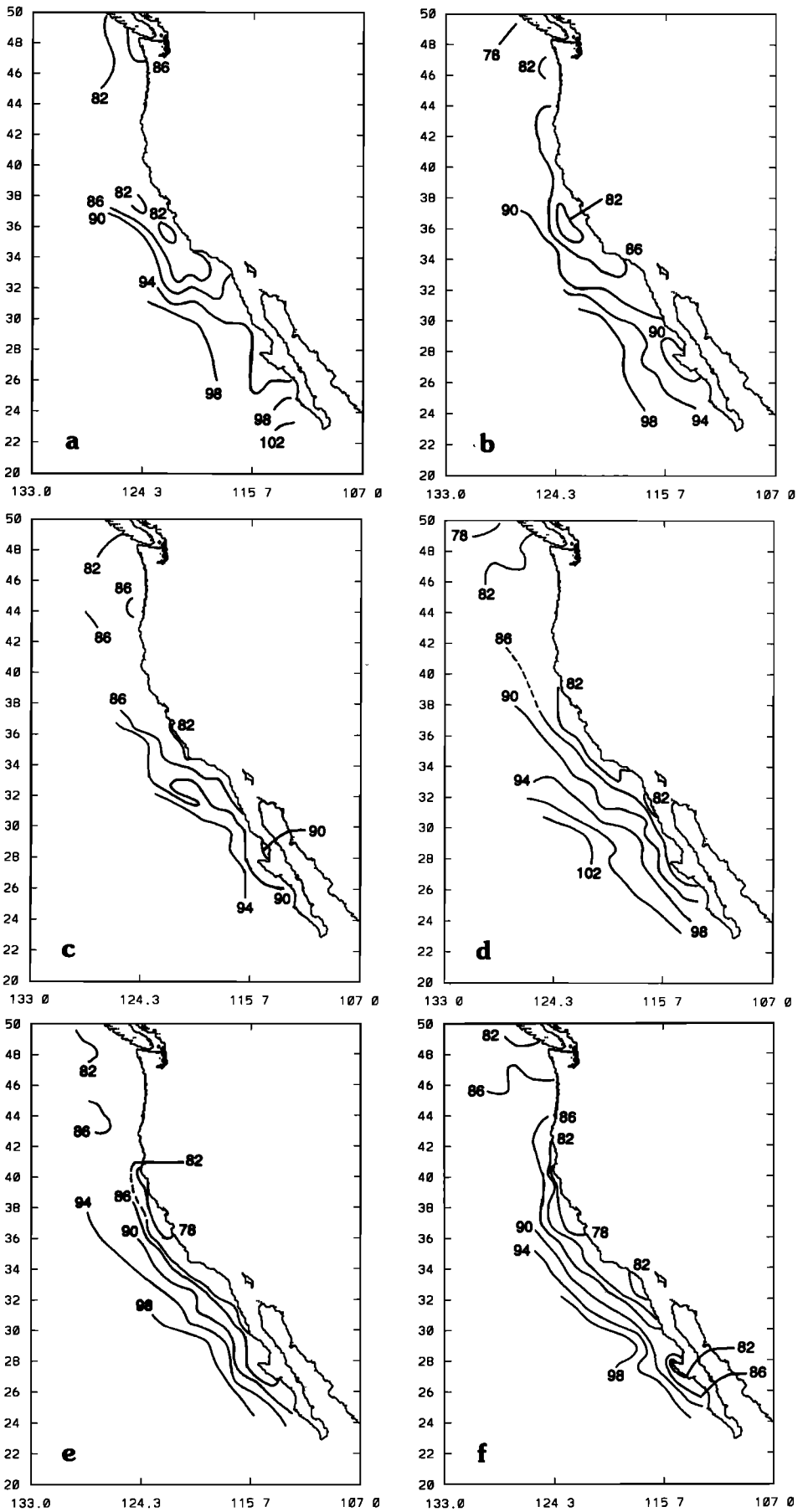

Figure 2. Dynamic height anomaly $\Delta\Phi$, 0/500 m. In these and in the following figures, the contour interval is 2 dyn. cm, dashed lines indicate areas of little or no data, and panels correspond to (a) January, (b) February, (c) March, (d) April, (e) May, (f) June, (g) July, (h) August, (i) September, (j) October, (k) November, and (l) December.

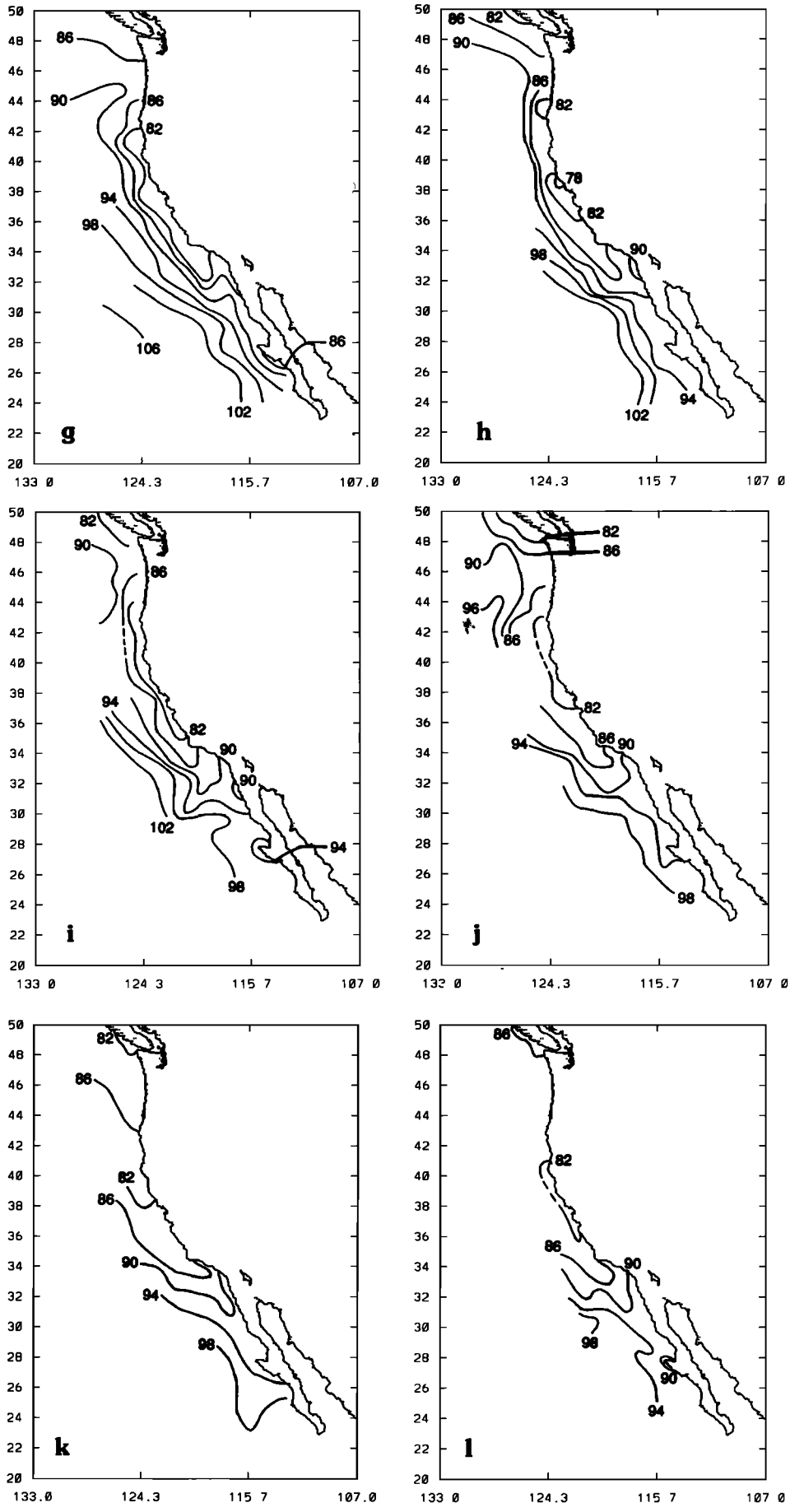

Figure 2. (continued)

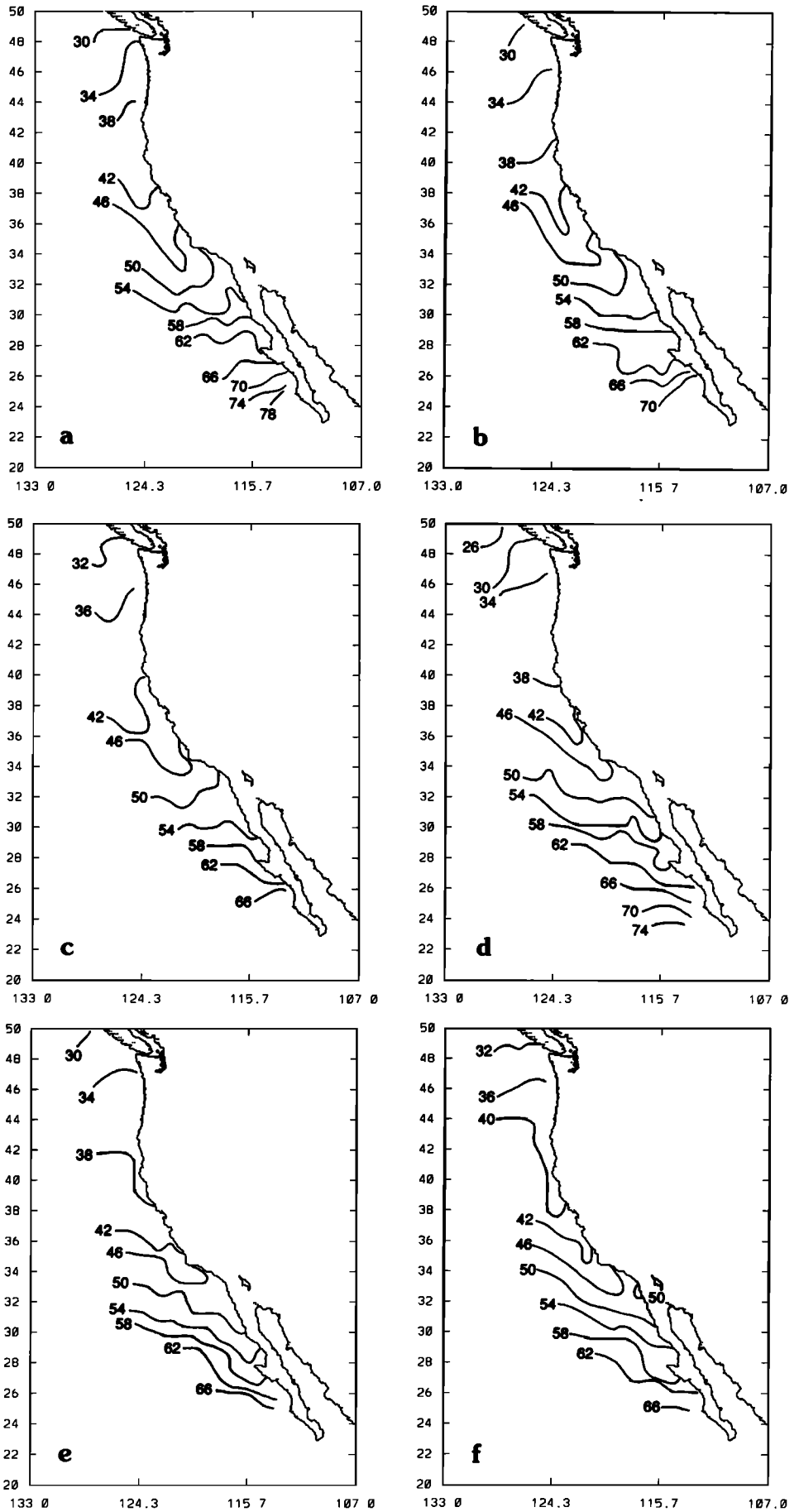

Figure 3. Dynamic height anomaly associated with temperature and pressure variability, calculated for salinity set to a constant value of 35 psu ($\Delta\Phi_{35TP}$), 0/500 m.

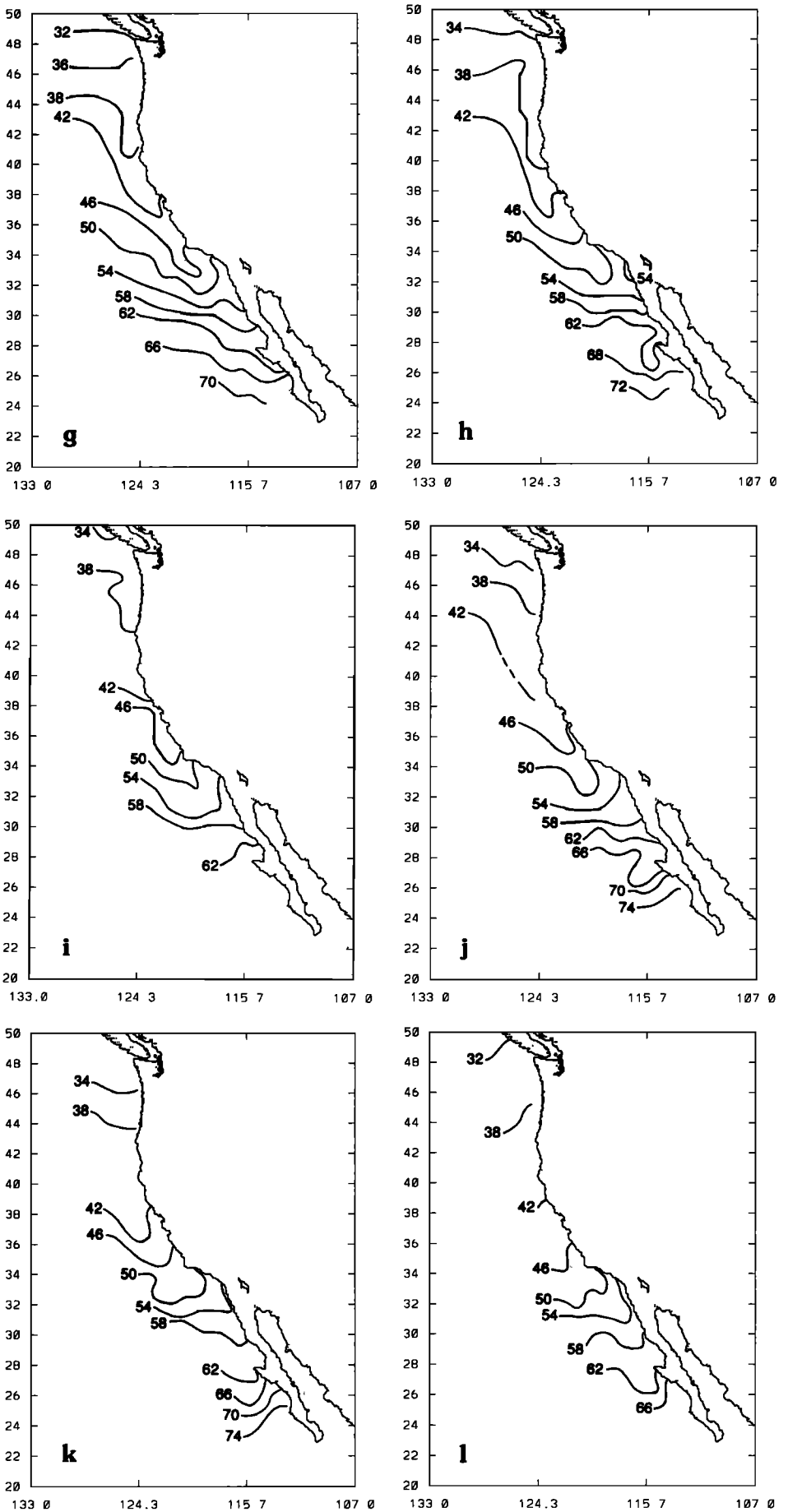

Figure 3. (continued)

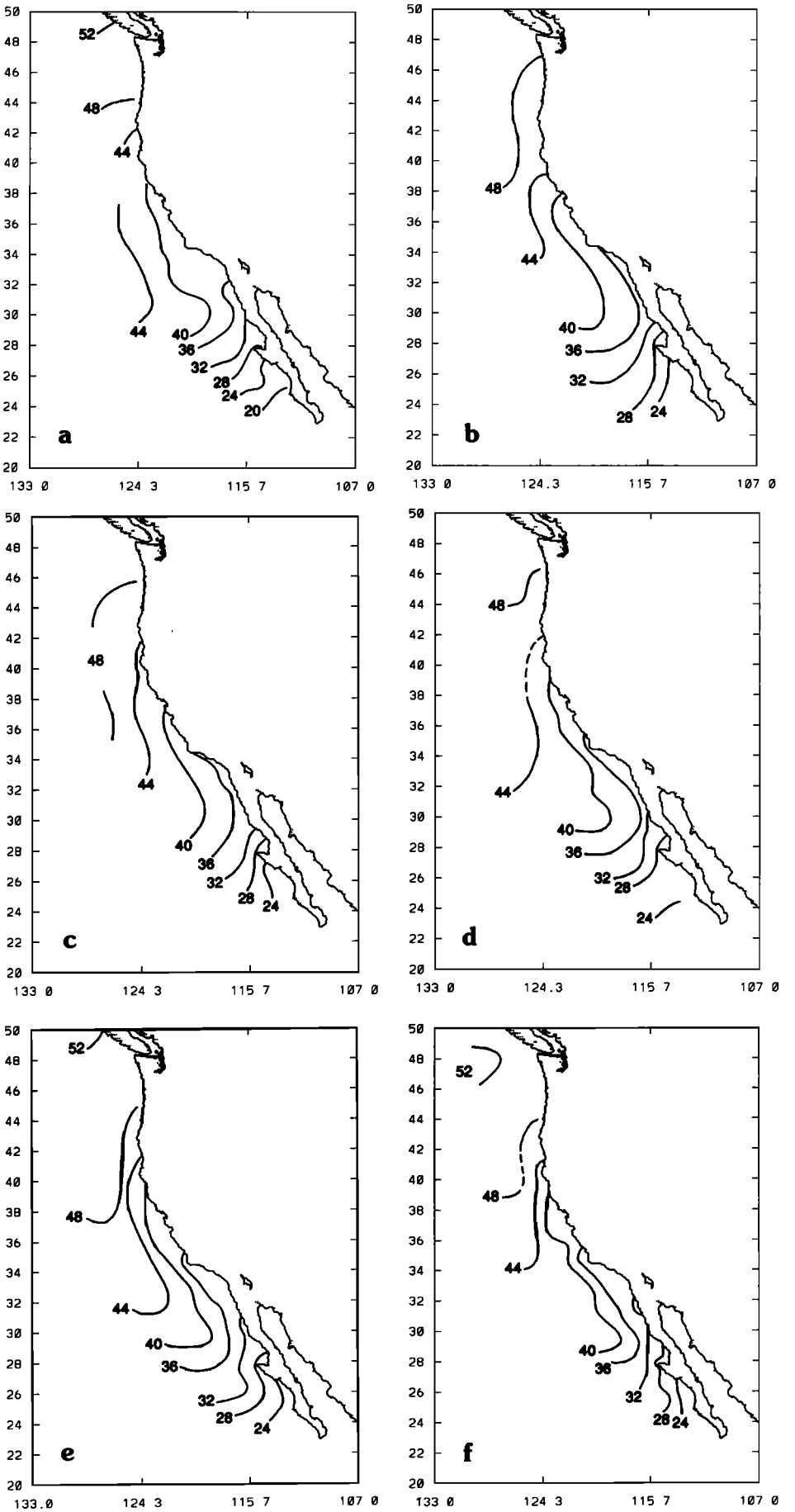

Figure 4. Dynamic difference fields $\Delta\Phi'$, 0/500 m.

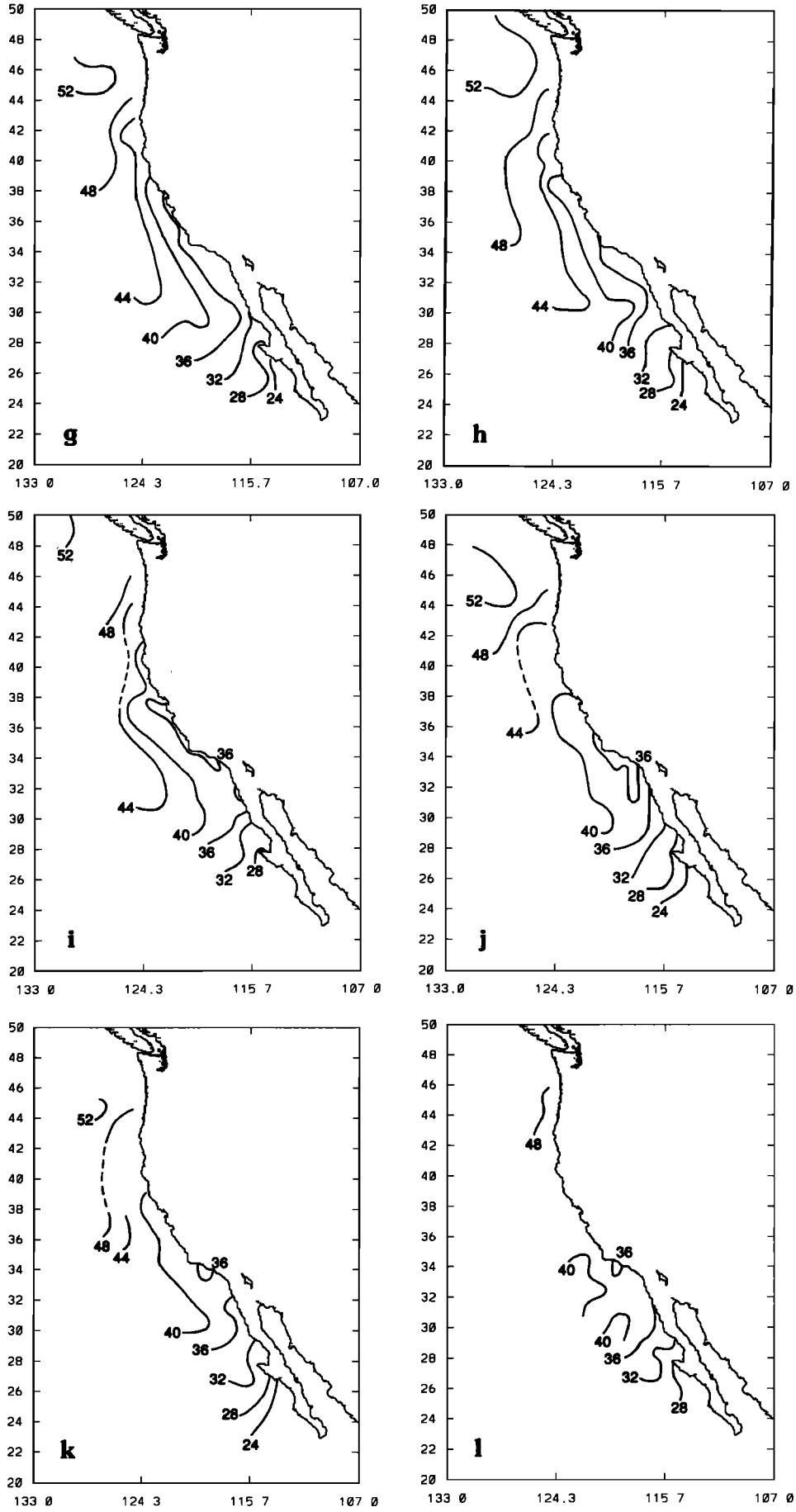

Figure 4. (continued)

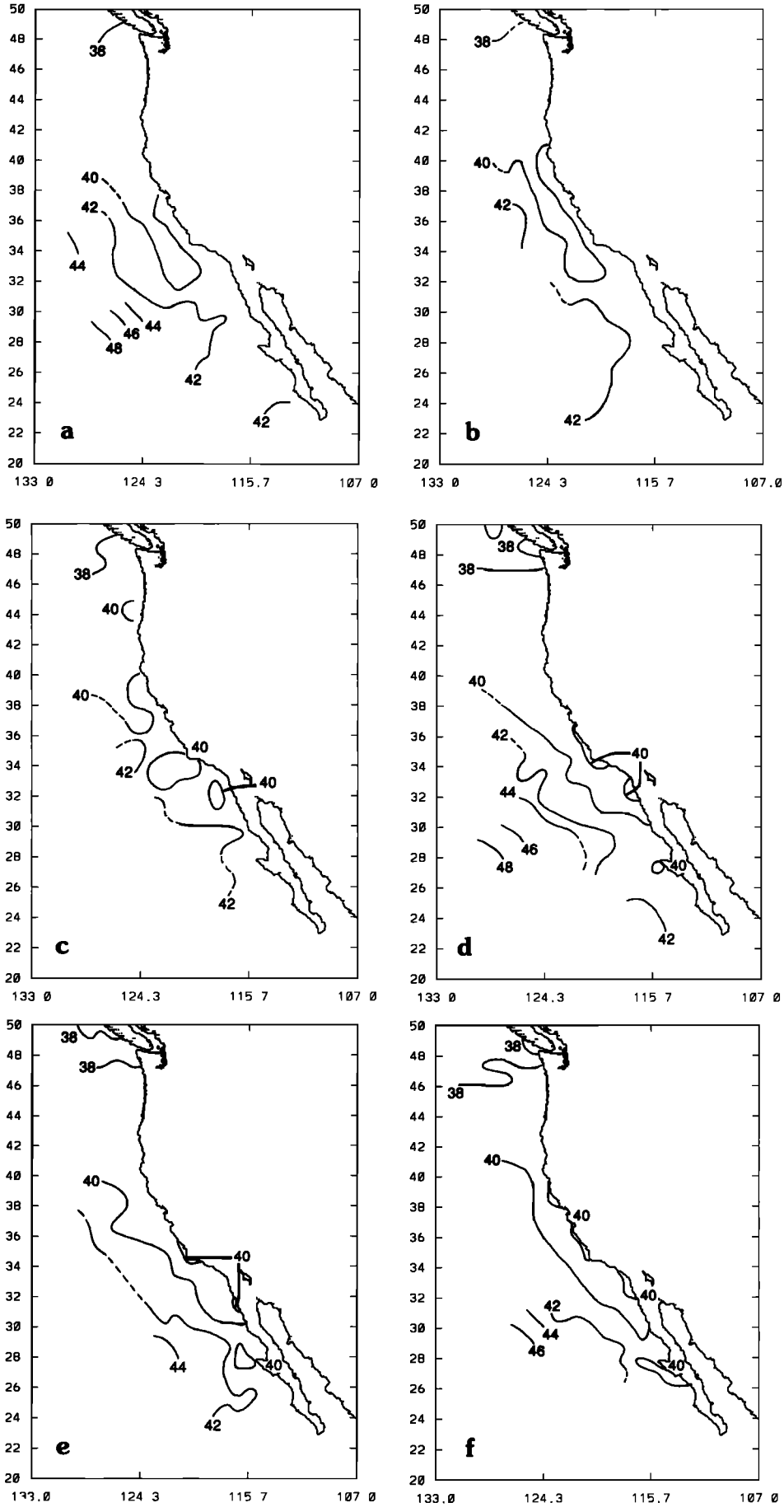

Figure 5. Dynamic height anomaly $\Delta\Phi$, 200/500 m.

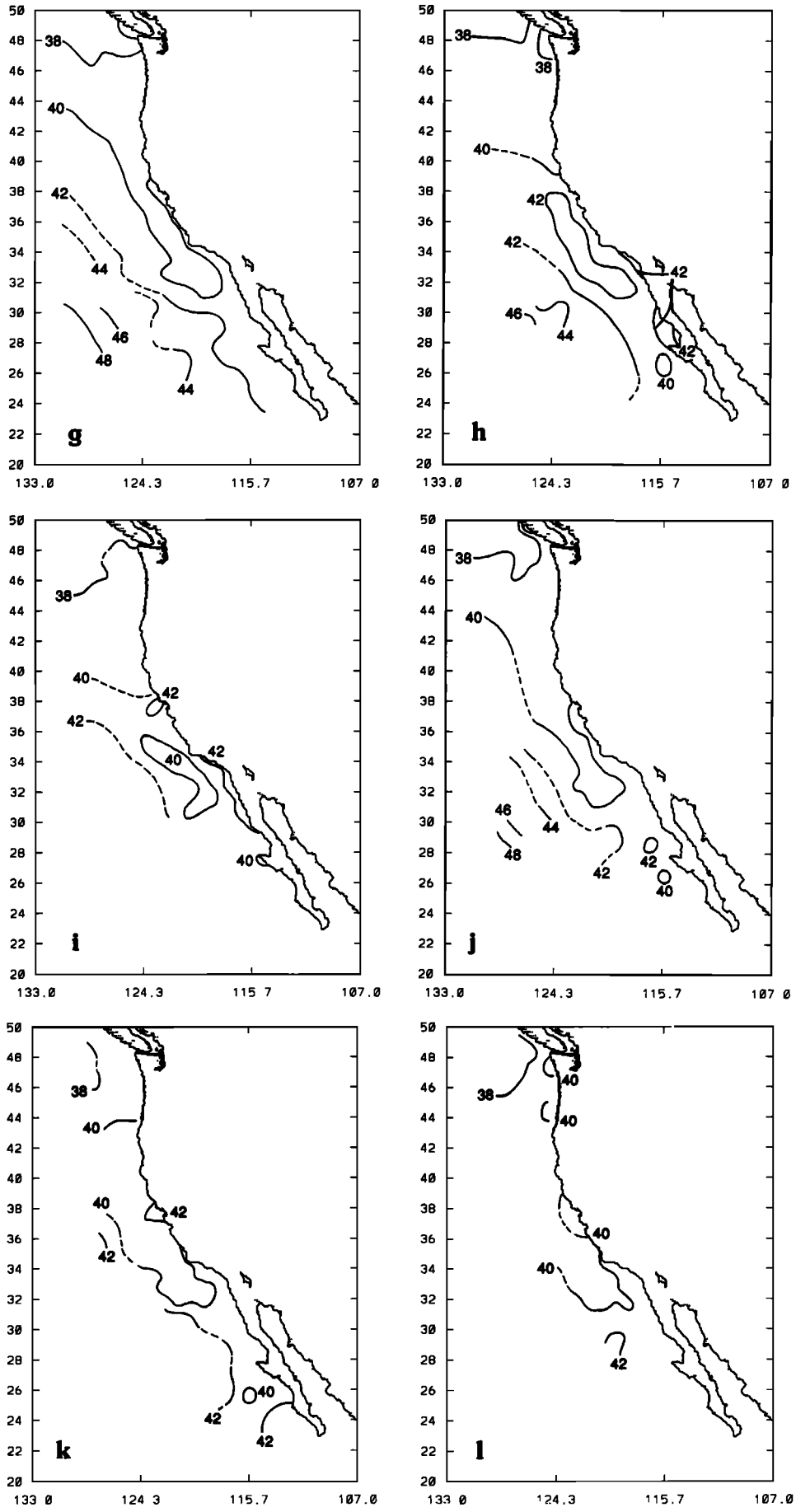

Figure 5. (continued)

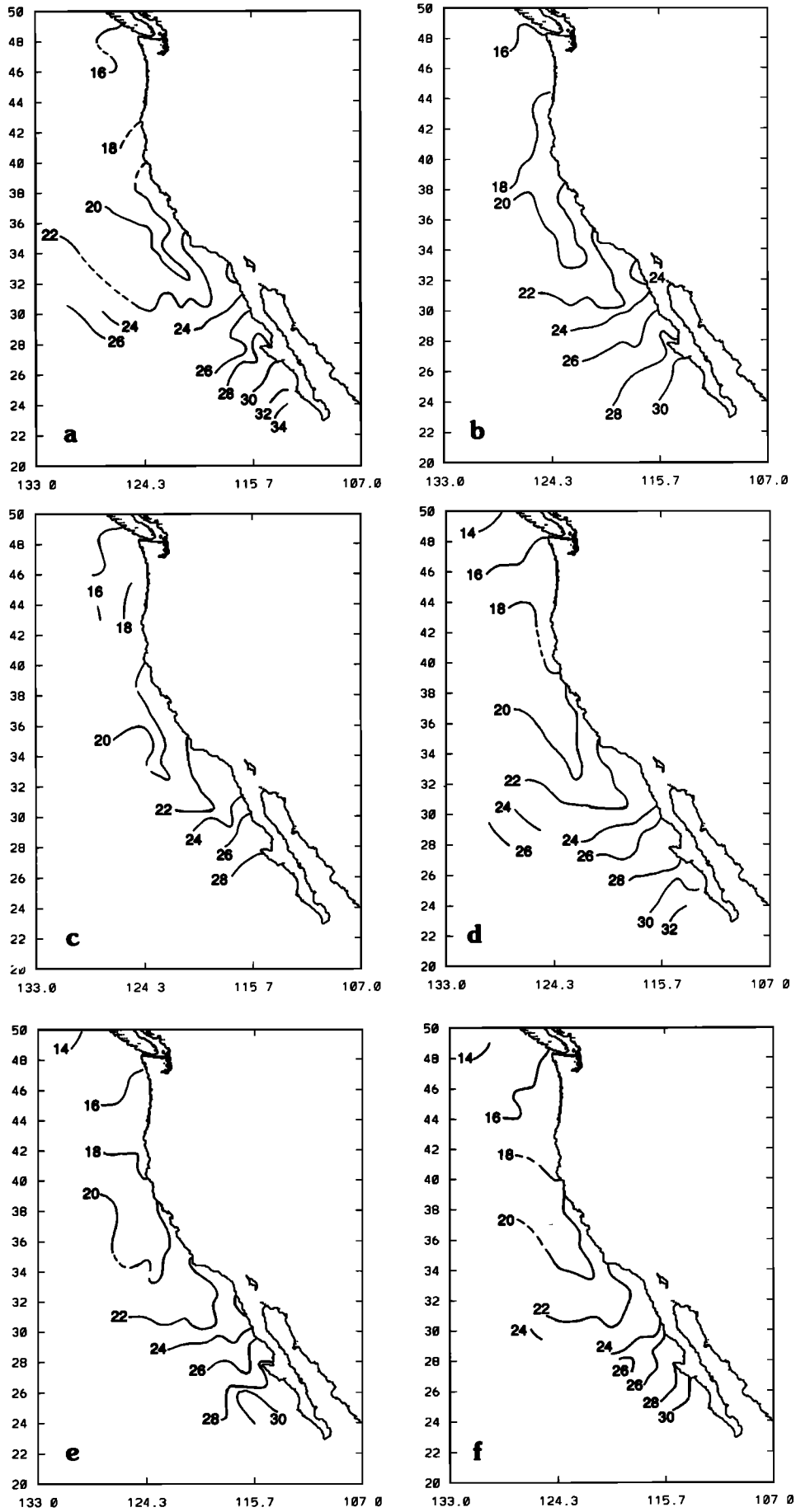

Figure 6. Dynamic height anomaly associated with temperature and pressure variability, calculated for salinity set to a constant value of 35 psu ($\Delta\Phi_{35TP}$), 200/500 m.

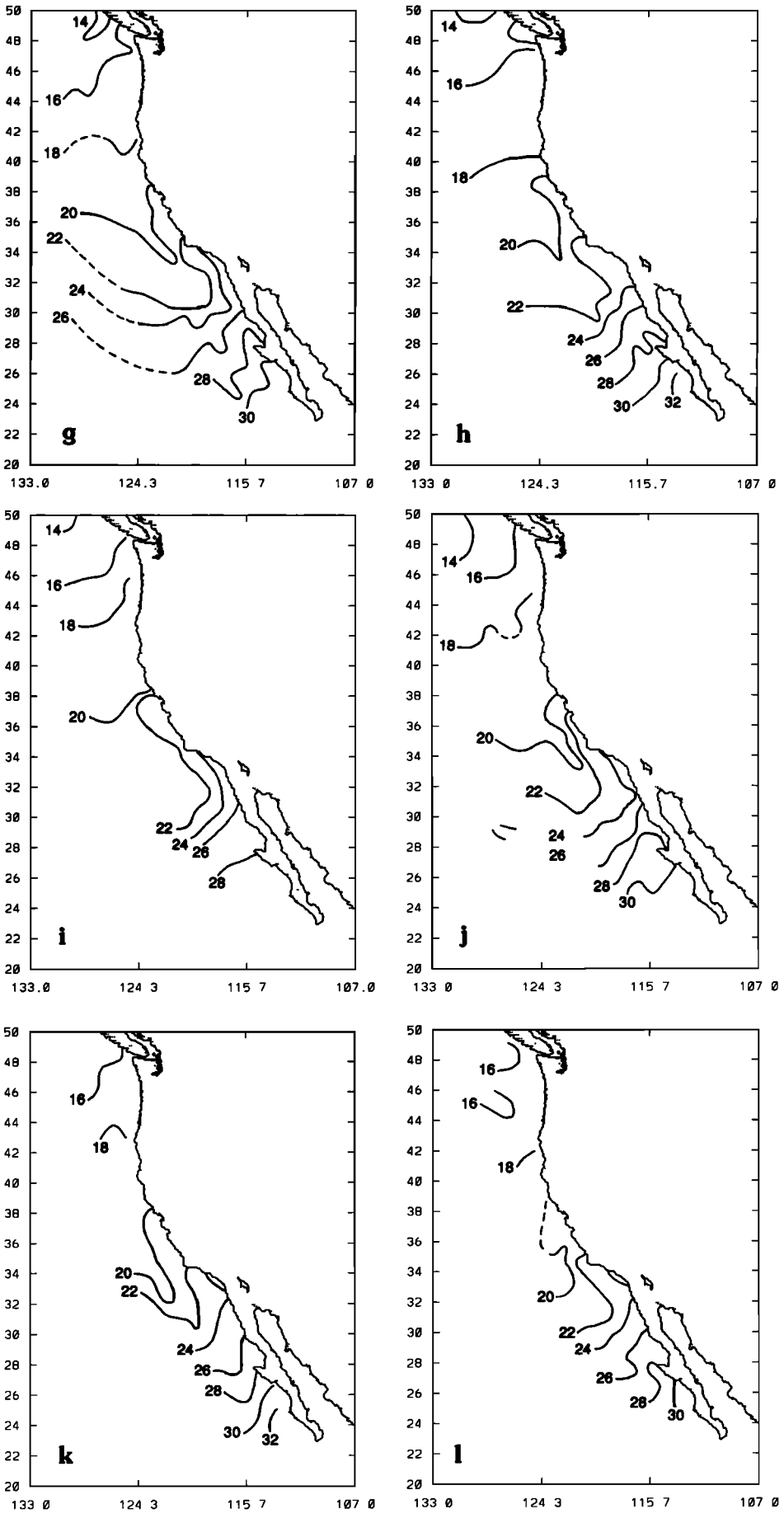

Figure 6. (continued)

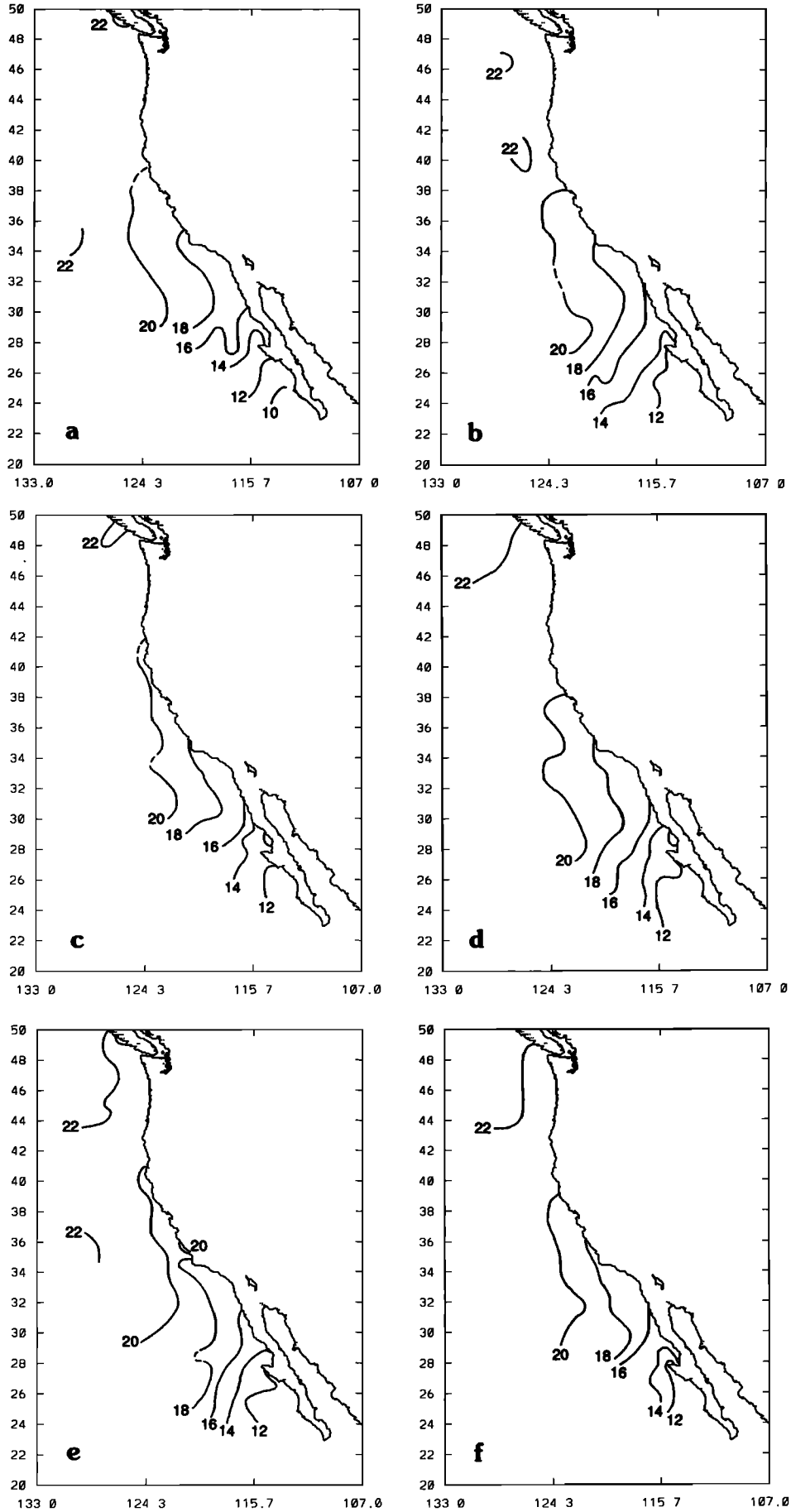

Figure 7. Dynamic difference fields $\Delta\Phi'$, 200/500 m.

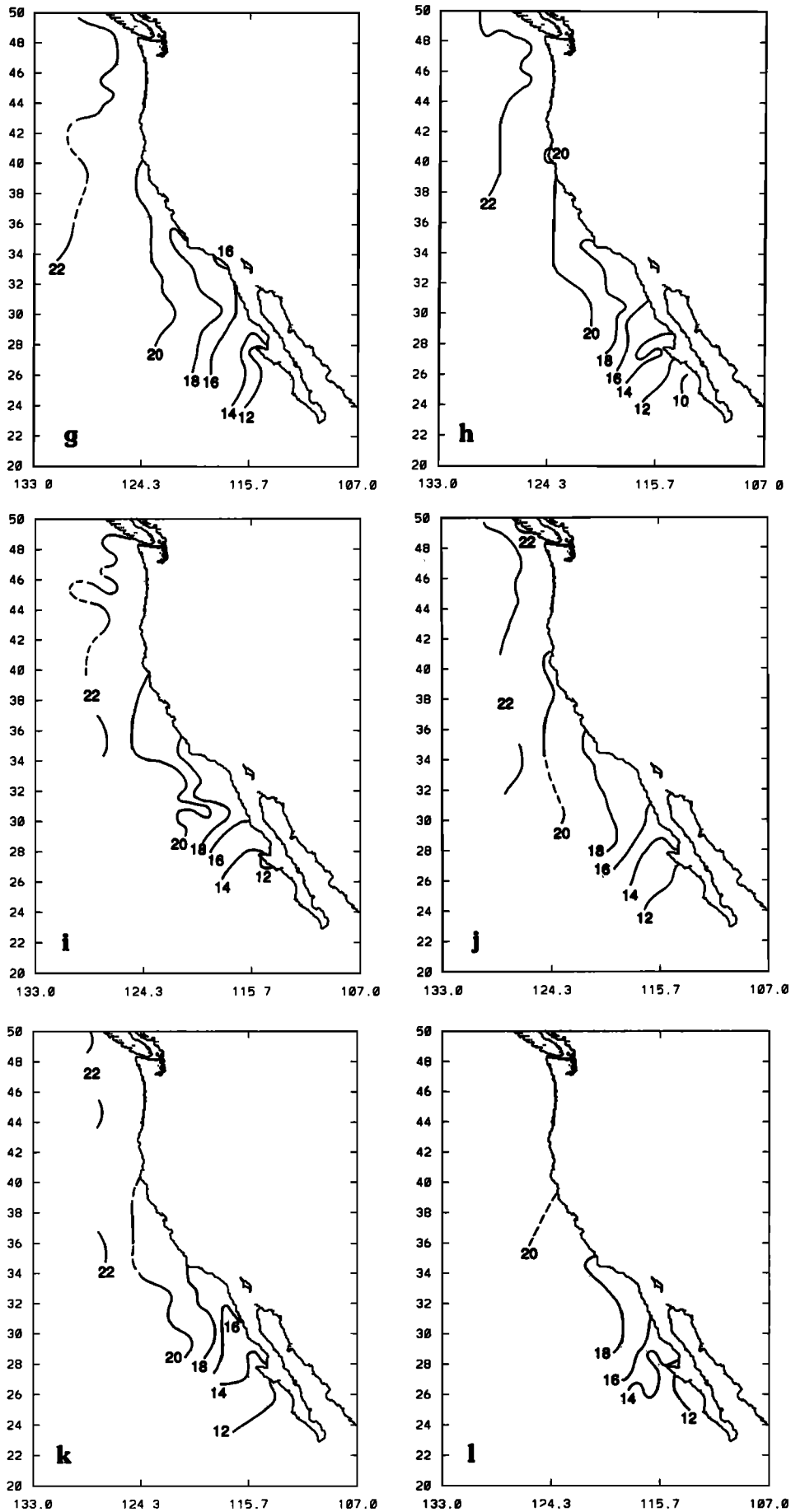

Figure 7. (continued)

from about 10 dyn. cm from Point Conception to Punta Eugenia. In a thermally driven system which was in geostrophic equilibrium, this would require flow into the coast in this region.

Off central and southern California, the 20 dyn. cm isostere is found. From January through August, and in October and November, this isostere indicates the development of a dynamic trough in this region, with assocated poleward flow at the coast. From February through August, the 22 dyn. cm isostere has a broader and weaker trough, possibly reflecting the pattern of the southern California eddy.

Analysis of the $\Delta\Phi'$ fields at 200/500 (Figure 7) shows that unlike the previous two fields, the isosteres associated with variable temperature and salinity decrease equatorward, from about 22 to 10 dyn. cm. The range, 12 dyn. cm, is almost as great as that due to variable temperature, 16 dyn. cm. As with temperature, the largest gradients occur in the region between Point Conception and Punta Eugenia, where the change amounts to about 10 dyn. cm. In this field, equatorward flow, away from the coast, occurs almost everywhere. A dynamic trough does not develop either off central California or in the region of the southern California eddy. Some indication of poleward flow at the coast can be found off northern Baja California in the November–February period.

5. Summary and Discussion

5.1. Summary

The monthly mean salinity field has been shown to have a pronounced effect on the large-scale geostrophic circulation of the CCS. Calculating dynamic height $\Delta\Phi$, by integrating δ over depth, and comparing it to $\Delta\Phi_{35TP}$, calculated by integrating δ_T, provided insight concerning the importance of salinity variation to the geostrophic flow field. The $\Delta\Phi$ results, where they overlap, are in very close agreement with *Wyllie* [1966]. At all depths the mean variability of salinity in the CCS is responsible for a significant equatorward component along the coast of California and a strong offshore component adjacent to Baja California.

The impact of salinity is complex and variable. In the region of the Columbia River's outflow, surface salinity may vary an entire practical salinity unit in 100 km, or 1 psu over the course of a year; yet in this region the depth-integrated importance of the salinity gradient is less important than anywhere else in the CCS. Off the coast of Baja California, where thermal expansion coefficients are high, saline contraction coefficients low, and surface salinity gradients have minimal impact on the density field, the importance of salinity variability 100 m below the surface is often equal to the importance of temperature variance. On the other hand, there seem to be regions of the order of 3° squares (e.g., in the central CCS region modeled by *Batteen et al.* [1989]) where the assumption of constant salinity might not cause significant errors in the estimation of density gradients. Areas where mean gradients in temperature and salinity have positive correlation in terms of their effects on density can border areas of negative covariance of the T-S gradients.

On the basis of these observations, it is reasonable to conclude that careful work concerning the CCS should include haline description. Descriptively and dynamically, both temperature and salinity are essential to accurately characterize the large-scale structure of the CCS.

5.2. Modeling Implications

Given that the effect of salinity is very important in the determination of the density field, can we accurately prescribe it, or should a fully active salinity field be used in dynamical models of the CCS? Here we consider several ways of prescribing the salinity field.

The effects of salinity on density might be achieved by using a temperature-driven linearization of density that simulates saline variability. For example, increasing the magnitude of the thermal expansion coefficient α in an upwelling process model may capture the effect of a positive T-S covariance on density. Entering different values of α for different regions and depths (higher values where covariance is positive, lower values where negative) would simulate salinity's variation over regions where salinity or temperature effects change sign. Use of a constant value of α over a range of temperatures, in addition to ignoring saline contributions, can superimpose a false smoothing tendency, resulting in an underestimation of the magnitude of positive $\Delta\rho$ in cold water, and negative $\Delta\rho$ in warm water. Forcing α to change more or less uniformly meridionally but at a higher rate than is warranted by the mean temperature gradient could allow study of the combined effects of meridional saline variation and smoothing.

Because salinity measurements are more expensive to make and more difficult to obtain than temperature observations, it may be desirable to estimate salinity from a known T-S correlation [*Stommel*, 1947]. *Emery* [1975] has shown that the accuracy of dynamic height calculations made from such derived salinities can, at least in some cases, be comparable to the accuracy of determinations made from observed salinities. In these cases, the salinity field in general can be inferred from XBT observations alone, as *Rienecker et al.* [1985] have attempted, or from conductivity-temperature-depth (CTD) casts (to convert XBT temperature profiles to density profiles) over a limited time period (~2 months) and a limited offshore spatial domain (~200 km square), as *Rienecker et al.* [1987] have attempted. In the latter case, the associated root-mean-square error in the surface height was estimated to be ~2 dyn. cm, compared with a typical dynamic range of 20 dyn. cm over the observational domain. We tried to apply the relationship *Rienecker et al.* [1987] used to larger regional models of the CCS and found that the resulting salinities were unrealistic, particularly in the coastal regions. This is not surprising, since the procedure, according to *Rienecker et al.* [1987], is most subject to error above 100 m depth, where the T-S correlation is more tight, and over the continental shelf and slope, where a change in the T-S relation may be expected.

The validity of such salinity inferences depends completely on the strength of the T-S correlation, or what *Stommel* [1947] called "range of uncertainty," i.e., the "tightness" of a particular T-S curve. This uncertainty in differential salinity can be related to

$$[(1 - r_{TS}^2) \times (\Delta S)^2]^{1/2}, \tag{3}$$

where ΔS is determined from the T-S curve, r_{TS} is the coefficient of determination for temperature and salinity, and $(1 - r_{TS}^2)$ is the fraction of salinity variance that cannot be explained by temperature variance. Clearly, the uncertainty increases as the strength of the correlation (and magnitude of r_{TS}^2) decreases. Therefore it may be reasonable to expect the

method of salinity inference from the T-S relationship to be most accurate in regions of highest T-S correlations and least accurate in regions where the T-S correlation is weak.

Investigations have been made to determine seasonal values of the T-S correlation (i.e., coefficients of determination) at 10-, 100-, 200-, and 500-m depth. The results (not shown) show the following: At 500-m depth, where one would expect the largest correlations, the coefficient of determination, r_{TS}, generally falls between -0.3 and 0.3, with larger absolute values usually occurring at the offshore edge of our data fields. At 200-m depth, r_{TS} south of 34°N and east of 118°W are generally positive (this is associated with changes in the shape of the T-S curve), while those elsewhere tend to be negative, and absolute values range to 0.8 at a few offshore locations. At 100-m depth the region of positive r_{TS} shrinks, owing in part to the influence of upwelling processes around Punta Eugenia, and a few values with an absolute value of 0.5 or 0.6 occur, usually at the offshore edge of our data base. At 10-m depth, most r_{TS} are negative in fall and winter, positive in spring, and negative along southern California in summer. The absolute values at 10-m depth are generally close to zero but range from 0.8 to 0.9 at some offshore grid points in the fall and winter.

In summary, the results show that most grid points have very low r_{TS} correlations. They also show that above 200-m depth, the T-S correlations change with depth, with geographical position, and with season.

These results strongly support the conclusions of *Blumberg et al.* [1984] that development of T-S curves for the CCS would not be cost effective for modeling efforts because of the lack of significant numbers of temperature observations below 200-m depth and because of relatively poor T-S correlations inherent in near-surface waters (less than 200-m depth). In the near-surface waters the poor correlations are likely due to a competition between the signature of the relatively cold and fresh Subarctic waters and the geostrophic adjustment associated with the acceleration of the California Current and upwelling. Additional problems in the CCS relate to the fact that the halocline coincides with a depth zone of little temperature change; below this depth a strong temperature-salinity contrast exists between North Pacific Intermediate Water and waters of equatorial origin.

For someone working with ocean temperature climatology in the CCS, our results could be used to derive a statistical relationship to infer dynamic heights from those computed using dynamic heights that have a constant salinity (e.g., S = 35). For example, a regression of $\Delta\Phi$ (0/500) to $\Delta\Phi_{35TP}$ (0/500) yields $\Delta\Phi$ (0/500) = 6.7 + 0.5$\Delta\Phi_{35TP}$ (0/500) with an rms error of 0.5 dyn. cm and a correlation coefficient of 0.75. The reason that these results are better than those derived from observations within a single grid point is that these fields are climatological, i.e., they have been averaged over time and space in contrast to data collected over limited temporal and spatial domains.

A modeler might be served as well by using a fully active salinity field as by attempting to prescribe the salinity field on the basis of its relationship with temperature. Likewise, an observationalist should probably use full CTD casts to determine the salinity in the CCS rather than use XBT observations to infer the salinity field. Our results quantify the improvement of the description of the kinematics of the CCS that salinity provides.

Acknowledgments. This work was done in the Department of Oceanography at the Naval Postgraduate School under the support of the Office of Naval Research and the National Science Foundation. Drafting of the figures by Mike Cook is greatly appreciated. Computer time was provided by the W. R. Church Computer Center at the Naval Postgraduate School. We wish to thank the reviewers for valuable comments on how to clarify the text.

References

Batteen, M. L., R. L. Haney, T. A. Tielking, and P. G. Renaud, A numerical study of wind forcing of eddies and jets in the California Current system, *J. Mar. Res.*, *47*, 493–523, 1989.

Blumberg, A. F., L. H. Kantha, H. J. Herring, and G. L. Mellor, California shelf physical oceanography circulation model, *Rep. 88*, vol. 1, 164 pp., Dynalysis of Princeton, Princeton, N. J., 1984.

Cooper, N. S., The effect of salinity on tropical ocean models, *J. Phys. Oceanogr.*, *18*, 697–707, 1988.

Emery, W. J., Dynamic height from temperature profiles, *J. Phys. Oceanogr.*, *5*, 369–375, 1975.

Emery, W. J., and J. S. Dewar, Mean temperature-salinity, salinity-depth and temperature-depth curves for the North Atlantic and the North Pacific, *Prog. Oceanogr.*, *11*, 219–305, 1982.

Gunderson, C. R., M. L. Batteen, and C. S. Nelson, Saline impact on the California Current system, *Tech. Rep. NPS 68-89-006*, 107 pp., Nav. Postgrad. Sch., Monterey, Calif., 1989.

Hickey, B. M., The California Current system—Hypotheses and facts, *Prog. Oceanogr.*, *8*, 191–279, 1979.

Huyer, A., Coastal upwelling in the California Current system, *Prog. Oceanogr.*, *12*, 259–284, 1983.

Huyer, A., and P. M. Kosro, Mesoscale surveys over the shelf and slope in the upwelling region near Point Arena, California, *J. Geophys. Res.*, *92*, 1655–1681, 1987.

Lynn, R. J., K. A. Bliss, and L. E. Eber, Vertical and horizontal distributions of seasonal mean temperature, salinity, sigma-t, stability, dynamic height, oxygen, and oxygen saturation in the California Current, 1950–1978, *CalCOFI Atlas 30*, 513 pp., Calif. Coop. Oceanic Fish. Invest., La Jolla, 1982.

Pickard, G. L., and W. J. Emery, *Descriptive Physical Oceanography*, 5th ed., 320 pp., Pergamon, New York, 1990.

Rienecker, M. M., C. N. K. Mooers, D. E. Hagan, and A. R. Robinson, A cool anomaly off northern California: An investigation using IR imagery and in situ data, *J. Geophys. Res.*, *90*, 4807–4818, 1985.

Rienecker, M. M., C. N. K. Mooers, and A. R. Robinson, Dynamical interpolation and forecast of the evolution of mesoscale features off northern California, *J. Phys. Oceanogr.*, *17*, 1189–1213, 1987.

Stommel, H., Note on the use of the T-S correlation for dynamic height anomaly computations, *J. Mar. Res.*, *6*, 85–92, 1947.

UNESCO, International Oceanographic Tables, vol. 4, *UNESCO Tech. Pap. Mar. Sci.*, *40*, 195 pp., 1987.

Wooster, W. S., and J. L. Reid Jr., Eastern boundary currents, in *The Sea*, vol. 2, *The Composition of Sea Water: Comparative and Descriptive Oceanography*, edited by M. N. Hill, pp. 253–280, Wiley-Interscience, New York, 1963.

Wyllie, J. G., Geostrophic flow of the California Current at the surface and at 200 meters, *CalCOFI Atlas 4*, 288 pp., Calif. Coop. Oceanic Fish. Invest., La Jolla, 1966.

M. L. Batteen, C. A. Collins, and C. S. Nelson, Department of Oceanography, Naval Postgraduate School, Monterey, CA 93943-5000. (e-mail: batteen@oc.nps.navy.mil)

C. R. Gunderson, Oceanography Department, U.S. Naval Academy, Annapolis, MD 21402.

(Received December 17, 1993; revised November 29, 1994; accepted December 28, 1994.)